Research Square

Preprints are preliminary reports that have not undergone peer review.
They should not be considered conclusive, used to inform clinical practice,
or referenced by the media as validated information.

Investigation of the Structure of the Joint Zone in Ti/Al/Aluminum Alloy Composites Produced by Explosive Welding with Ultrasonic Treatment

Evgeniy Kuzmin
Mikhail Korolev
mihakorolew@mail.ru

Volgograd State Technical University: Volgogradskij gosudarstvennyj tehniceskij universitet
https://orcid.org/0000-0002-2430-6384
Valentin Kharlamov
Sergei Kuzmin
Vladimir Lysak

Research Article

Keywords: explosive welding, ultrasound, EBSD, FIB, dynamic recrystallization

Posted Date: March 17th, 2026

DOI: https://doi.org/10.21203/rs.3.rs-9091619/v1

License: This work is licensed under a Creative Commons Attribution 4.0 International License.
Read Full License

Version of Record: A version of this preprint was published at The International Journal of Advanced Manufacturing Technology on June 25th, 2026. See the published version at https://doi.org/10.1007/s00170-026-18580-x.

Investigation of the structure of the joint zone in Ti/Al/Aluminum alloy composites produced by explosive welding with ultrasonic treatment

Authors: Evgeniy Kuzmin, Mikhail Korolev*, Valentin Kharlamov, Sergei Kuzmin, Vladimir Lysak
Volgograd State Technical University, Lenin av. 28, Volgograd 400005, Russia
* Corresponding author.
E-mail address: mihakorolew@mail.ru (M.P. Korolev).

Abstract: The article presents the results of a study of the microstructure of the near-boundary regions of aluminum and the aluminum-magnesium alloy AMg6 in three-layer titanium-aluminum-aluminum alloy composites obtained by explosive welding with ultrasonic treatment. Using electron backscatter diffraction (EBSD) and focused ion beam (FIB) electron microscopy, it is shown that the AMg6 alloy exhibits a finer grain structure than pure aluminum. Directly at the interface with aluminum in AMg6, a recrystallized layer with a grain size of 0.2-0.3 μm was formed. The application of ultrasound during welding contributed to an increase in the thickness of the recrystallized layer in AMg6 from 1.7-1.9 μm to 5.4 μm. In the pure aluminum layer, the ultrasonic treatment facilitated grain refinement at the interface with the titanium layer, while a decrease in the density of low-angle boundaries was observed at the interface with AMg6.

Keywords: explosive welding, ultrasound, EBSD, FIB, dynamic recrystallization

1. Introduction

Due to their high specific strength and corrosion resistance, titanium and aluminum alloys are widely used in high-tech industries. Joints of titanium with aluminum alloys make it possible to effectively combine the high strength of titanium with the low density and relatively low cost of aluminum. These materials are used in aircraft construction, rocket engineering, automotive manufacturing, shipbuilding, and other fields [1, 4, 5, 6]. Recently, the development of titanium-aluminum armor plates has also been advancing [2, 3]. To produce joints between titanium and aluminum alloys, methods such as diffusion welding [1], hot rolling [4], friction stir welding [5], laser welding [6], and explosive welding are employed. Explosive welding offers distinct advantages over other methods for producing such materials due to the high quality of the joints, relatively low cost, the ability to weld large-thickness and large-area joints, as well as the absence of a need for expensive equipment and complex tooling.

However, explosive welding of dissimilar materials, such as titanium and aluminum alloys, presents certain challenges. Due to the relatively high hardness

of aluminum alloys (compared to aluminum), they require greater energy expenditure for plastic deformation and joint formation during explosive welding. At the same time, an excessive increase in collision energy leads to the formation of a layer of molten metal at the interface and cracks in the near-boundary region of the aluminum alloy [7]. The melted areas are also a source of microcracks due to the formation of brittle intermetallic compounds of the Ti-Al system within them [8, 9]. The difference in thermal conductivity and coefficient of thermal expansion between titanium and aluminum leads to the formation of residual stress fields in the bimetal [10, 11], which also deteriorates the properties of the joints. Malakhov et al. [11] investigated the strength of titanium-AMg6 joints and concluded that the low strength was associated with low deformation during welding; however, increasing the welding parameters can promote the formation of melted areas, which also degrades the joint properties. Wu et al. [12] reported that during the welding of TA2 titanium with 5083 aluminum alloy, delamination and continuous interlayers of molten metal formed at the interface. For effective welding of these materials, the authors proposed using an intermediate aluminum layer. Li et al. [13] studied the mechanical properties of explosively welded TA1 and 5083 joints and showed that the melted layer is a site for crack initiation due to the presence of brittle intermetallics within it. Bi et al. [14] concluded that during explosive welding of TA2 titanium with 5083, the intermetallic compound Ti_3Al formed in the melted zones, which contributed to crack formation at the interface. To prevent this phenomenon, the authors proposed using vacuum welding or employing an intermediate layer.

These and other problems mean that direct welding of titanium to aluminum alloys is rarely used in practice. Most often, an intermediate layer of pure aluminum is used for welding these materials. Pure aluminum, due to its low hardness and high ductility, welds well by explosion even with relatively low energy input, and the use of a thin intermediate layer makes it possible to reduce the energy released at the interface of dissimilar materials [12, 15]. Fang et al. [15] showed that during direct welding of TA2 to 5083, microcracks and continuous interlayers of molten metal form at the joint interface; however, adding an intermediate layer allows solving the problem of excessive kinetic energy loss during direct welding, improving weldability, and obtaining defect-free joints. Wu et al. [12] drew similar conclusions. Gałka & Najwer [16] presented the results of a study on the features of explosive welding of the Ti6Al4V titanium alloy with the AA2519 aluminum alloy and concluded that directly welded joints, although possessing high strength, have low ductility and are prone to cracking during straightening; therefore, using an intermediate aluminum layer during welding is

the optimal solution. Thus, welding through a pure aluminum interlayer is currently the preferred technological option for joining titanium with aluminum alloys, as it can ensure a defect-free microstructure and good mechanical properties of the joints, which are sufficient for most applications.

One of the ways to further improve explosive welding technology could be the application of combined methods, such as welding with simultaneous ultrasonic treatment. Ultrasonic vibrations are successfully used to improve the quality of welded joints in various welding methods, such as gas-shielded welding [17], laser welding [18], friction stir welding [19], and others. The specifics of applying ultrasonic vibrations in different processes vary significantly, and depending on the welding method, it may involve increasing the arc efficiency, the effect of ultrasound on the weld pool melt, changes in friction conditions, etc.

In explosive welding, ultrasonic vibrations act on one of the plates being welded, inducing a standing wave within it. The influence of ultrasound on metal in the solid phase helps to reduce the metal's resistance to deformation [20] (acoustoplasticity) and lower the level of residual stresses [21]. Currently, there is no complete and universally accepted theory describing the mechanism behind the observed effects. The main approaches to this issue suggest that the acoustoplastic effect contains various components and may be associated with thermal softening [22], the superposition of alternating and static stresses [23], as well as an increase in dislocation mobility and enhanced dipole annihilation processes [24]. From a microstructural perspective, ultrasonic treatment can promote enhanced recrystallization and grain refinement [25]; however, there is also evidence that at low deformation, dislocation density may decrease [26]. Therefore, there is reason to believe that the influence of ultrasound on the microstructure depends on many factors, including the material properties and the degree of deformation.

This paper examines the effect of ultrasonic treatment on the microstructure of the near-boundary regions of materials when welding the VT1-0 + A5 + AMg6 joint. Previous studies have demonstrated that the application of ultrasound to the base plate during explosive welding helps to expand the weldability window, reduce the amount of molten metal at the interface, and increase the strength of the joint [27]. This study focuses on investigating the changes in the grain structure of materials during welding with ultrasonic treatment.

2. Materials and Methods

The materials studied were commercially pure titanium VT1-0, commercially pure aluminum grade A5, and the aluminum-magnesium alloy AMg6. The chemical composition of the materials is given in Table 1. Explosive

welding was carried out using a parallel arrangement (simultaneous detonation) scheme (Fig. 1). The AMg6 plate, with overall dimensions of 200×80×5.8 mm, served as the base plate. A titanium plate with dimensions of 260×150×4 mm was used as the flyer plate, and a sheet of commercially pure aluminum, measuring 240×120×1 mm, served as the intermediate layer. Two methods of introducing ultrasound to the welded plates were considered: application to the base AMg6 plate and application to the commercially pure aluminum intermediate layer.

Table 1. Chemical composition of the materials (mass fraction, %)

	Ti	Al	Mg	Si	Fe	Cu	Mn	Zn
VT1-0	base	-	-	0.1	0.25	-	-	-
A5	0.02	base	0.03	0.25	0.3	0.02	0.05	0.06
AMg6	0.02-0.1	base	5.8-6.8	0.4	0.4	0.1	0.5-0.8	0.2

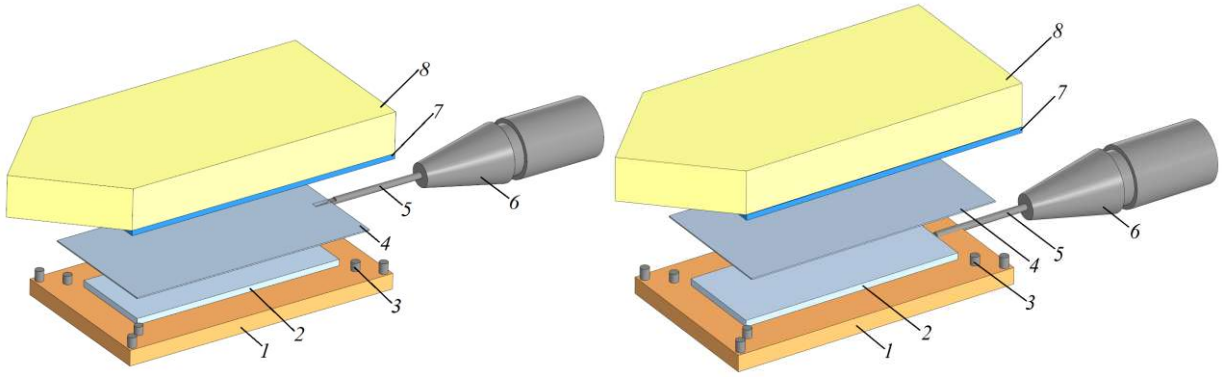
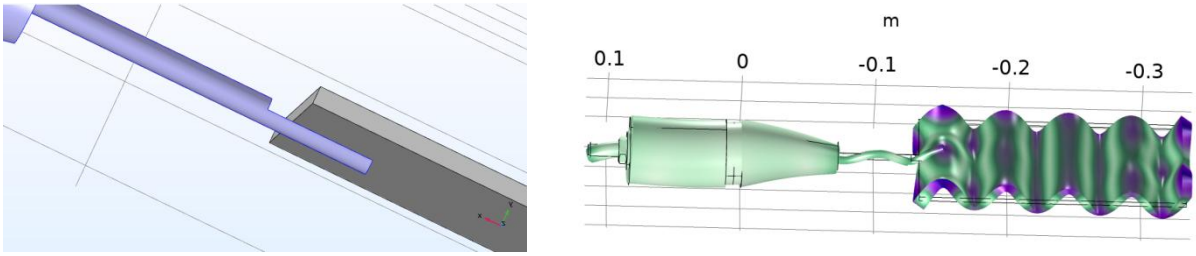


Fig. 1. Assembly diagram for welding with ultrasonic treatment: (a) - application of ultrasound to the intermediate layer; (b) - application of ultrasound to the base plate; 1 - anvil; 2 - base plate (AMg6); 3 - welding gap; 4 - aluminum intermediate layer; 5 - waveguide (sonotrode); 6 - ultrasonic transducer; 7 - flyer plate (VT1-0); 8 - explosive charge.

Ultrasonic vibrations in the plate were excited using an ultrasonic piezoelectric transducer connected to the plate via a waveguide with a diameter of 6 mm. The vibration frequency was approximately 18 kHz, the displacement amplitude at the end of the ultrasonic transducer was ≈ 4 μm, and the duration of ultrasonic treatment prior to welding was about 5 seconds. The method of application used ensures the formation of a standing wave of a flexural mode in the plate, an example of which is shown in Fig. 2.



a) b)

Fig. 2. Method of connecting the waveguide to the plate (a) and an example of a flexural vibration mode (b)

The calculated parameters of the explosive welding are given in Table 2. Ammonite 6ZhV (21% TNT and 79% ammonium nitrate according to GOST 21984-76) was used as the explosive, mixed with sand, which acts as an inert filler that reduces the detonation velocity. The methodology for calculating the regimes is based on a two-dimensional model of a metal plate accelerated by expanding detonation products, using semi-empirical relationships describing the characteristics of the explosive mixtures. The parameter W_2 characterizes the amount of energy expended on the plastic deformation of the surfaces of the welded plates during explosive welding. A detailed description of the calculation of this value is given in [28].

Table 2. Explosive welding parameters

Materials	Thickness, mm	Explosive mixture (ammonite No. 6GV/sand)	Charge height, mm	Collision point velocity, m/s	Welding gap, mm	Collision velocity, m/s	Collision angle, °	Energy W_2, MJ/m^2
VT1-0 + A5 + AMg6	4 + 1 + 5,8	60/40	40	2105	2	439	11,98	0,19
					1	392	10,68	0,57

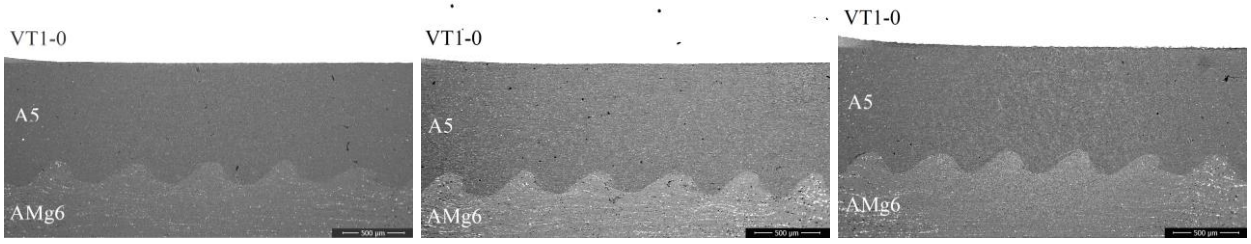
The choice of welding mode is determined by the properties of the explosive, the thicknesses of the welded plates, and the specific features of welding three-layer joints. The selected mode is near the lower limit of the weldability window and ensures the minimum necessary level of plastic deformation at the titanium-aluminum interface, which makes it possible to achieve a joint with strength equal to that of the base materials while minimizing structural heterogeneity at the interface between the materials. Three series of experiments were carried out: in the first, ultrasonic vibrations were introduced into the base

AMg6 plate; in the second, ultrasound was applied to the intermediate aluminum layer; and in the third, welding was performed without ultrasound.

After welding, samples were cut from the center of the plates and subjected to a standard preparation procedure for microscopic examination. Microstructural analysis using SEM, FIB, and EBSD methods was performed using an FEI Versa 3D DualBeam electron microscope.

3. Results and Discussion

All three series of samples were successfully welded. To assess their mechanical properties, a pull-off strength test of the layers was conducted. The test results showed that failure of the joints occurred in a ductile manner through the aluminum layer, with the joint strength ranging between 85-95 MPa, exceeding the strength of the aluminum in its initial state. All joints exhibited a similar microstructure at both interfaces (Fig. 3). A flat interface profile was formed in the titanium-aluminum bonding zone. In the sample welded without ultrasound, a small number of melted metal inclusions, 5-7 μm thick, were present at the titanium-aluminum interface. At the interface between the aluminum interlayer and the AMg6 layer, a wavy profile with a wavelength of approximately 570-610 μm and an amplitude of 170-180 μm was formed in all joints.



a) b) c)

Fig. 3 Wave profile at the interface of VT1-0+A5+AMg6 joints welded without ultrasound (a), with ultrasound applied to the base plate (b), and to the intermediate layer (c)

For a detailed study of the material structure near the joint interface, an investigation was carried out using electron backscatter diffraction (EBSD). Figure 4 shows IPF maps of the microstructure of the aluminum layer in the region adjacent to the titanium bonding zone, where black lines indicate grain boundaries with a misorientation angle >10° (high-angle boundaries).

The results of the study revealed a significant difference in the structure of the near-interface aluminum regions between the samples. During welding without ultrasound, the structure of the aluminum near the interface can be categorized into into regions with different grain structures. At a distance > 40 μm from the titanium interface (Fig. 4, a), the original grain boundaries are discernible in the aluminum; however, the accumulation of plastic deformation within the grains led

to the appearance of subgrains and an increase in misorientation between them. At a distance of 15 to 40 μm from the interface, the aluminum exhibits a fibrous structure formed by elongated grains up to 9 μm thick, with inclusions of fine grains approximately 2 μm in size. At the interface with titanium, there is a layer of fine-grained aluminum about 10-15 μm thick with a grain size of 1.5-2.5 μm. It is likely that the formation of the fine-grained structure resulted from dynamic recrystallization occurring in this region, the localized nature of which was associated, on the one hand, with the localization of plastic deformations, and on the other hand, with the need to achieve critical strain for the initiation of dynamic recrystallization [29].

The application of ultrasound during welding to the base AMg6 plate also affected the structure of the aluminum interlayer at the interface with titanium (Fig. 4, b). In the near-interface zone, one can also distinguish an area of recrystallized grains at the boundary, an area of elongated grains, and an area of deformed original grains. However, compared to welding without ultrasound, polygonization of the original structure is more pronounced throughout the entire studied area. According to the EBSD mapping results, the total length of boundaries with a misorientation angle >10° in the studied area was greater than in the control sample, amounting to 5.91 mm, compared to 3.64 mm (without ultrasound).

During welding with ultrasound applied to the intermediate aluminum layer (Fig. 4, c), the outlines of the original grains or distinct boundaries between areas with different grain sizes or shapes were practically not discernible in the aluminum structure; instead, an almost uniform structure formed throughout the entire studied area, consisting of recrystallized grains and subgrains with sizes of about 0.5-3.5 μm. The total length of high-angle boundaries in the studied area was the highest among all samples, amounting to 7.43 mm. The observed grain refinement can be explained by the influence of acoustic oscillations. Previously, works [25, 30, 31, 32] have shown that the application of ultrasound to metal during deformation promotes grain refinement. The mechanism of this phenomenon is associated with an increase in the density and mobility of dislocations under the action of ultrasonic vibrations, which facilitates the dynamic recrystallization process and leads to the formation of a fine-grained structure [25, 30].

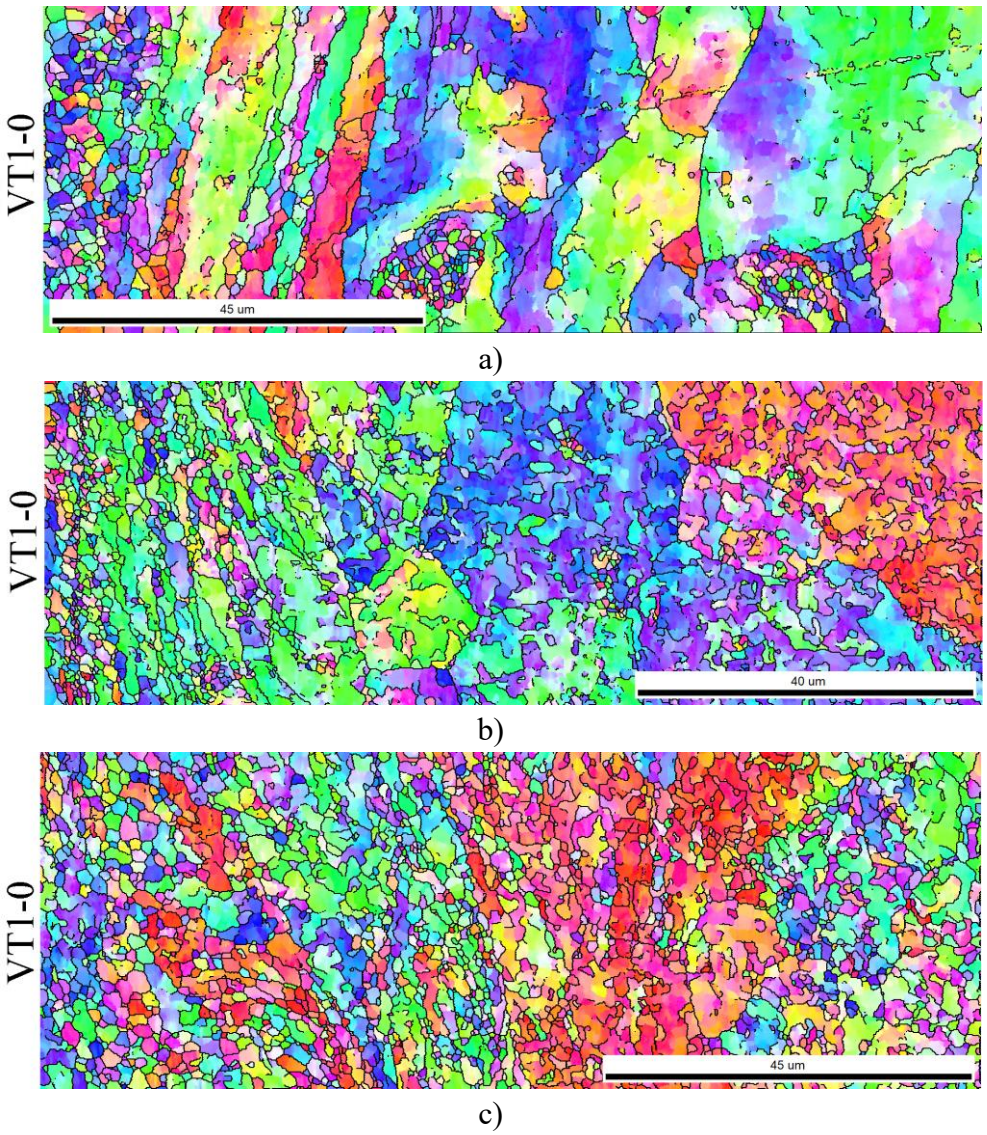


Fig. 4 IPF maps of the aluminum layer in the region adjacent to titanium. Black lines indicate grain boundaries with a misorientation angle >10°: a - welding without ultrasound; b - ultrasound applied to the base AMg6 plate; c - ultrasound applied to the intermediate A5 layer.

A study of the material structure at the aluminum-AMg6 interface was also conducted. The welding conditions at this interface were significantly different. The energy expended on plastic deformation was considerably higher, yet the difference in the mechanical properties of the welded materials was smaller. A wavy profile formed at the interface, instead of the flat interface between titanium and aluminum, which likely also affected the distribution pattern of plastic deformation. In all cases, the area selected for the study was located in a trough of the wave profile, where the interface between the materials was flattest.

Figure 5 shows IPF+IQ maps of the near-interface regions of A5 aluminum and AMg6. The different colors indicate the crystallographic orientation (IPF map), and the gray shades show the image quality (IQ) of the diffraction patterns. It is worth noting that there is a noticeable difference between the aluminum and

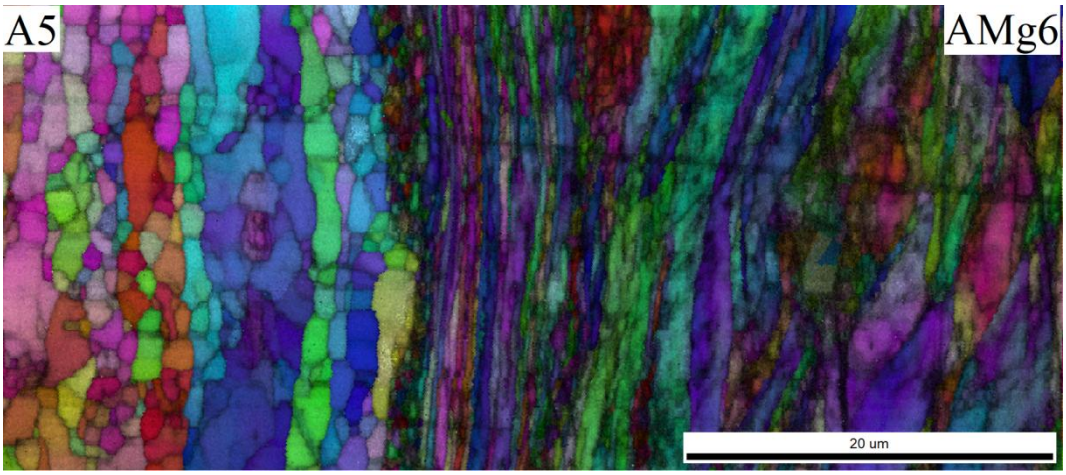
the aluminum alloy in the figures, causing AMg6 to appear much darker than the aluminum. According to literature data, such contrast in IQ maps is most often associated with grain boundaries, crystal lattice distortions, dislocation clusters, and other factors [33]. Therefore, it is likely that the observed difference between aluminum and AMg6 is related to the presence of alloying elements in the aluminum alloy, a higher dislocation density, and a smaller grain size in AMg6. It should also be specifically noted that, despite the aluminum and AMg6 deforming together, a finer structure formed in AMg6 than in pure aluminum. This result clearly demonstrates how differently deformation proceeds in aluminum and the aluminum alloy. Previously, in studies focused on severe plastic deformation methods, many researchers have noted a connection between the content of alloying elements and the grain refinement of aluminum alloys during deformation. The reasons for this are commonly explained by the influence of dissolved alloying elements and second-phase particles, which hinder dislocation movement, contribute to an increase in dislocation density, and promote the occurrence of dynamic recrystallization [34, 35].

Fig. 5, a shows an IPF+IQ map of the near-interface regions of aluminum and AMg6 in a joint welded without ultrasound exposure. In the aluminum near the interface, a structure is observed consisting of elongated (deformed) grains ranging from 1 to 6 μm in width, fragmented into subgrains with a non-equiaxed shape. As a result of deformation, some subgrains increased their angular misorientation, transforming into individual grains with a size of 1-2 μm. In AMg6, directly at the interface, a layer 1-2 μm thick formed, consisting of fine recrystallized grains. Beneath it lies a zone up to 10 μm deep with a fibrous microstructure, composed of highly elongated grains 0.2-0.5 μm thick, stretched parallel to the interface.

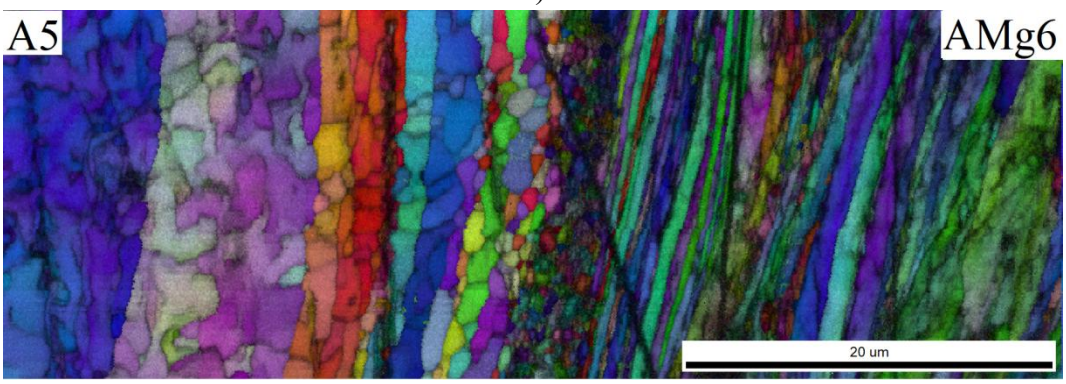
During welding with ultrasound applied to the base AMg6 plate (Fig. 5, b), structural changes were observed both in the aluminum alloy itself, which was subjected to ultrasound, and in the aluminum interlayer. The structure of the near-interface aluminum layer, as in the control sample, consisted of elongated grains with a developed substructure, whose thickness ranged from 2 to 9 μm. However, polygonization and the increase in misorientation within the original grains were less pronounced, and the formation of a fine-grained structure occurred predominantly in a layer 4-5 μm thick near the interface. The structure of AMg6 was generally similar to the structure welded without ultrasound exposure discussed earlier; the only significant difference was an increase in the thickness of the recrystallized AMg6 at the interface to 3-4 μm. This indicates that ultrasound, acting directly on the stronger AMg6, reduces its resistance to deformation, which

leads to the localization of large strains in the near-interface region and more active recrystallization.

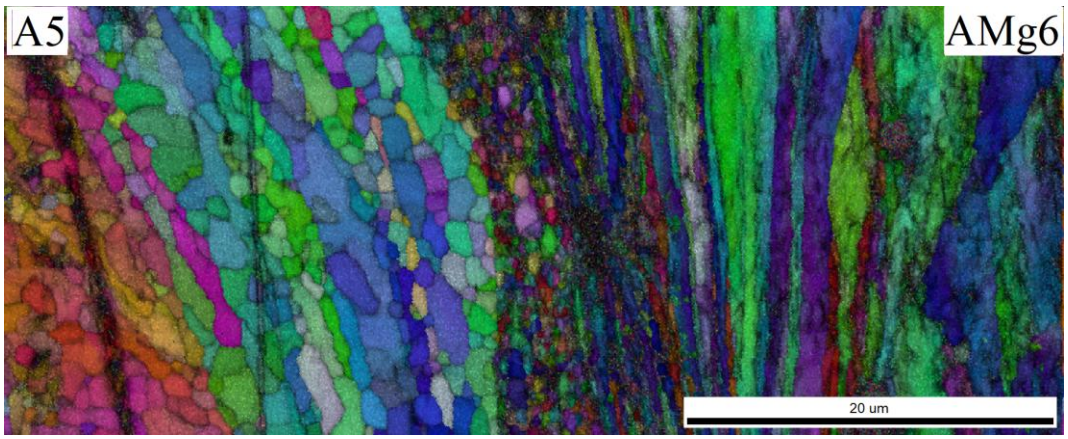
During welding with ultrasound applied to the aluminum layer (Fig. 5, c), the structure of the aluminum in the studied area was practically indistinguishable from that observed during welding without ultrasound. It is worth noting that, unlike the interface with titanium, where the application of ultrasound to the aluminum layer caused the most significant structure refinement (Fig. 4c), the structure of the aluminum at the interface with AMg6 changed only slightly. This is likely due to the different deformation conditions at this interface, resulting from a smaller difference in the physical and mechanical properties of the metals being deformed, different collision velocity and energy W_2, and the presence of a wave profile. In AMg6, the application of ultrasound led to an increase in the thickness of the recrystallized layer compared to conventional welding, reaching 4-4.5 μm.



a)



b)

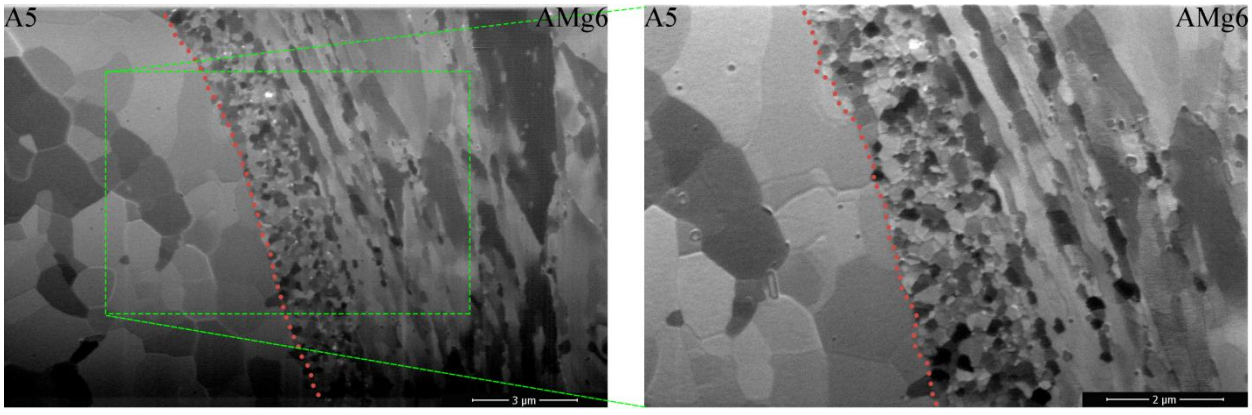


c)

Fig. 5 IPF+IQ maps of the aluminum-AMg6 interface: a - welding without ultrasound; b - ultrasound applied to the base AMg6 plate; c - ultrasound applied to the intermediate A5 layer.

For a more detailed study of the recrystallized layer at the aluminum-AMg6 interface, an investigation was carried out using focused ion beam (FIB) scanning. This research method allows observation of grain boundaries and crystal lattice orientation due to the interaction of the gallium ion beam with the crystal lattice of the sample [36]. The study was conducted in "ion wells" – cross-sections on the sample surface created by ion milling.

Figure 6 shows images of the grain structure of the near-interface regions of aluminum and AMg6, where the interface between the materials is highlighted in color. In the sample welded without ultrasound (Fig. 6, a), the thickness of the recrystallized layer was 1.7-1.9 μm, and the grain size was about 0.2-0.3 μm. In the sample welded with ultrasound applied to the base AMg6 plate (Fig. 6, b), the thickness of the recrystallized layer was significantly larger, varying in the range from 3.7 to 5.4 μm. The grain sizes in this layer varied over a wider range, from 0.2 to 0.5 μm. During welding with ultrasound applied to the intermediate layer (Fig. 6, c), the thickness of the fine-grained layer was 4-4.5 μm, and the grain size also lay in the range of 0.2-0.5 μm.



a)

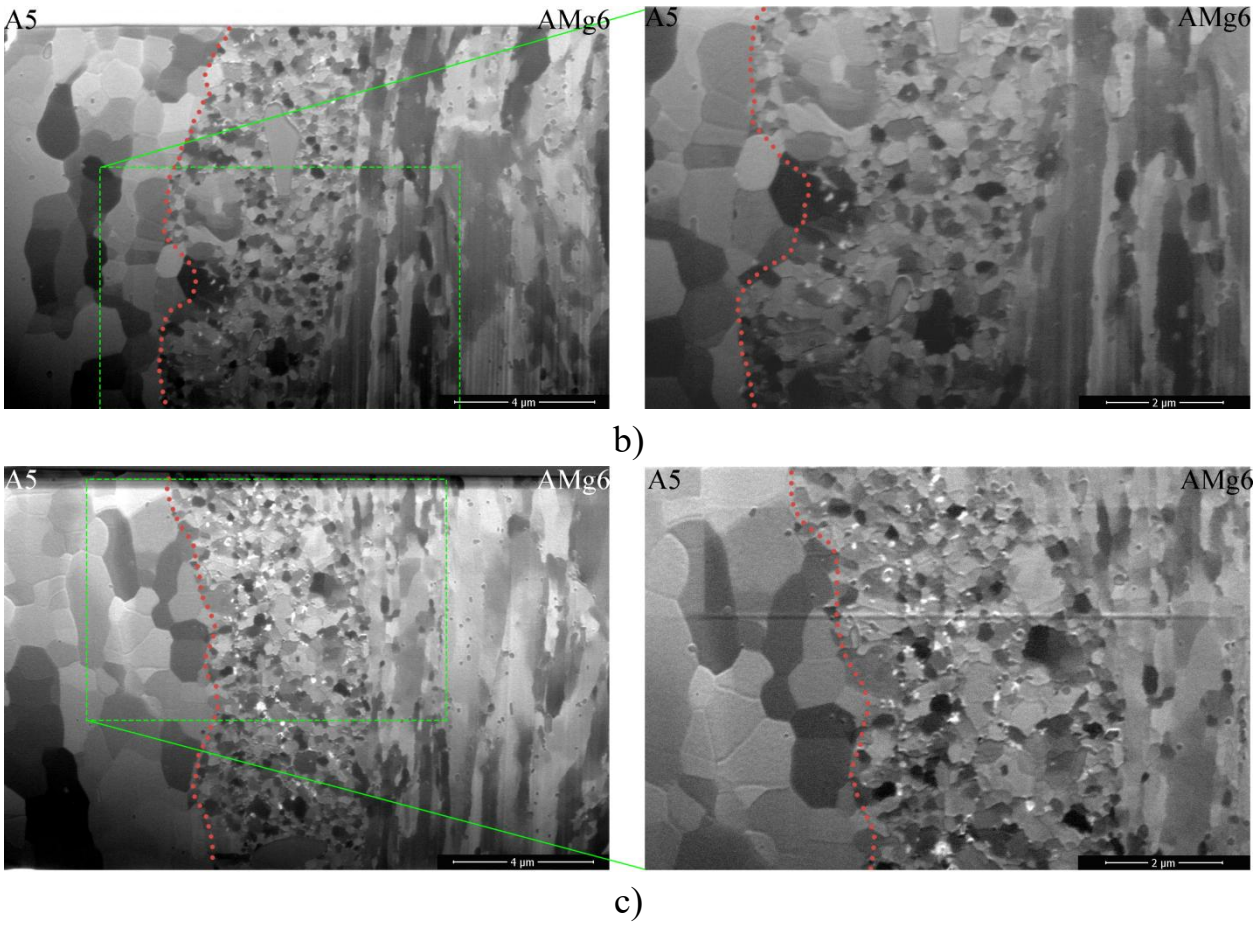


Fig. 6 Images of the grain structure at the aluminum-AMg6 interface obtained by ion beam scanning: a - welding without ultrasound; b - ultrasound applied to the base AMg6 plate; c - ultrasound applied to the intermediate A5 layer.

4. Conclusion

The microstructural studies revealed occurring in the near-interface regions of aluminum and the aluminum alloy during explosive welding with simultaneous exposure to ultrasonic vibrations. The application of ultrasound contributed to the refinement of the aluminum structure at the interface with titanium, with the most pronounced effect observed when ultrasound was applied directly to the aluminum layer. The study was conducted to a depth of up to 115 μm, and throughout this depth, the disappearance of original grain boundaries, enhanced polygonization, and increased misorientation between subgrains with the formation of new grains of 1-2 μm in size were observed. The total length of boundaries with a misorientation angle >10° in the studied near-interface area increased from 3.64 mm during welding without ultrasound to 7.43 mm during welding with ultrasound applied to the aluminum.

In aluminum at the interface with AMg6, such significant structural changes were not observed; on the contrary, when ultrasound was applied to the base AMg6 plate, a decrease in the number of subgrains was observed in the near-

interface regions of the aluminum. Most likely, this is related to the redistribution of strain fields. Ultrasound, by reducing the deformation resistance of AMg6, causes a larger portion of the plastic deformation to localize in AMg6 rather than in aluminum, which explains the lesser structural changes in the latter.

In AMg6, regardless of the method of introducing the vibrations, the application of ultrasound promoted dynamic recrystallization in the near-interface region, which was manifested in an increase in the thickness of the recrystallized layer at the interface with aluminum. The most pronounced effect of ultrasound was observed when vibrations were applied directly to the AMg6 plate, resulting in an increase in the thickness of the recrystallized layer from 1.7-1.9 μm in the joint welded without ultrasound to 3.7-5.4 μm in the sample welded with ultrasound applied to the base AMg6 plate.

Acknowledgments

The research was carried out at the expense of the grant of the Russian Science Foundation No. 25-29-00609, https://rscf.ru/project/25-29-00609/

Declaration of conflicting interest

The authors report there are no competing interests to declare.

Data availability

The data that support the findings of this study are available from the corresponding author, upon reasonable request.

References

1. Wang, Y., Zhao, W., Zhang, B., et al. Enhanced interfacial properties and deformation behavior of Ti/Al composite plates through pure Al interlayer-Assisted diffusion bonding. *Mater Sci Eng A* 944, 148947 (2025). https://doi.org/10.1016/j.msea.2025.148947
2. Cai, Y., Wu, X., Shi, C., et al. Explosive welding of TA2-SiC-AW5083 composite armor. *Compos Sci Technol* 257, 110799 (2024). https://doi.org/10.1016/j.compscitech.2024.110799
3. Akgül, A., Durgutlu, A., Karakoç, H., et al. Ballistic and interfacial properties of Al-Ti armor materials produced by explosive welding. *Int J Adv Manuf Technol* 141, 1677–1703 (2025). https://doi.org/10.1007/s00170-025-16801-3
4. Gao, B., Hao, Y., Yu, C., et al. Study on temperature control and bonding properties of Ti/Al composite plates rolled by differential temperature rolling with mobile induction heating. *J Manuf Process* 134, 348-359 (2025). https://doi.org/10.1016/j.jmapro.2024.12.054

5. Li, B., Zhang, Z., Shen, Y., et al. Dissimilar friction stir welding of Ti–6Al–4V alloy and aluminum alloy employing a modified butt joint configuration: Influences of process variables on the weld interfaces and tensile properties. *Mater Des* 53, 838-848 (2014). https://doi.org/10.1016/j.matdes.2013.07.019
6. Zheng, ZM., Zhang, J. & Xing, YZ. A review on controlling the formation of intermetallic compounds in Ti/Al dissimilar metal laser weld seams. *Weld World* (2025). https://doi.org/10.1007/s40194-025-02198-w
7. Korolev, M.P., Kuz'min, E.V., Lysak, V.I., et al. Structure and Properties of Titanium/Aluminum–Magnesium Alloy Explosive Welds. *Russ Metall* 2024, 1084–1090 (2024). https://doi.org/10.1134/S0036029524702057
8. Hu, X., Liu, Y., Wu, Y., et al. Microstructure and In Situ Tensile Mechanical Properties of Ti/Al3Ti Composites Prepared by "Explosive Welding + Heat Treatment". *Trans Indian Inst Met* 77, 821–830 (2024). https://doi.org/10.1007/s12666-023-03105-x
9. Wang, J., Li, Xj., Yan, Hh., et al. Experimental and Numerical Simulation Study on Microstructural Defect Control at Ti/Al Explosive Welding Clad Plates Interface. *JOM* 77, 1816–1824 (2025). https://doi.org/10.1007/s11837-025-07129-0
10. Fronczek, D., Saksl, K., Chulist, R., et al. Residual stresses distribution, correlated with bending tests, within explosively welded Ti gr. 2/A1050 bimetals. *Mater Charact* 144, 461-468 (2018). https://doi.org/10.1016/j.matchar.2018.08.004
11. Malakhov, A., Saikov, I., Denisov, I., et al. AlMg6 to Titanium and AlMg6 to Stainless Steel Weld Interface Properties after Explosive Welding. *Metals* 10, 1500 (2020). https://doi.org/10.3390/met10111500
12. Wu, X., Shi, C., Fang, Z., et al. Comparative study on welding energy and Interface characteristics of titanium-aluminum explosive composites with and without interlayer. *Mater Des* 197, 109279 (2021). https://doi.org/10.1016/j.matdes.2020.109279
13. Li, Z., Lin, Y.C., Zhang, L., et al. In-situ investigation on tensile properties of a novel Ti/Al composite sheet. *Int J Mech Sci* 231, 107592 (2022). https://doi.org/10.1016/j.ijmecsci.2022.107592
14. Bi, ZX., Li, XJ., Zhang, TZ., et al. Microstructure and characterization of Ti–Al explosive welding composite plate. *Int J Adv Manuf Technol* 123, 1825–1833 (2022). https://doi.org/10.1007/s00170-022-10027-3

15. Fang, Z., Shi, C., Sun, Z., et al. Influence of interlayer technique on microstructure and mechanical properties of Ti/Al cladding plate manufactured via explosive welding. *Mater Res Express* 6, (2019). https://doi.org/10.1088/2053-1591/ab42ac
16. Gałka, A. & Najwer, M. Explosive Cladding of Titanium and Aluminium Alloys on the Example of Ti6Al4V-AA2519 Joints. *Arch Metall Mater* 60, (2015). https://doi.org/10.1515/amm-2015-0477
17. Liao, H., Zhao, X., Liu, Y., et al. Investigation of optimizing mechanical properties of 441 stainless steel welded joints via the synchronous ultrasound radiation assisted TIG welding. *J Mater Res Technol* 37, 929-937 (2025). https://doi.org/10.1016/j.jmrt.2025.05.215
18. Li, L., Deng, P., Tan, Y., et al. Enhancing impact toughness in 904L stainless steel welded joints using ultrasound-assisted laser welding without sacrificing the strength and ductility. *J Mater Res Technol* 36, 4476-4489 (2025). https://doi.org/10.1016/j.jmrt.2025.04.112
19. Zhao, W., Wu, C. & Shi, L. Acoustic induced antifriction and its effect on thermo-mechanical behavior in ultrasonic assisted friction stir welding. *Int J Mech Sci* 190, 106039 (2021). https://doi.org/10.1016/j.ijmecsci.2020.106039
20. Siu, K.W., Liu, H. & Ngan, A.H.W. A universal law for metallurgical effects on acoustoplasticity. *Materialia* 5, 100214 (2019). https://doi.org/10.1016/j.mtla.2019.100214
21. Zha, F.C., Wang, Y.Q., Liu, Z.H., et al. Experimental and numerical study on residual stresses relief in 316 L austenitic stainless steel welded joints using layer-by-layer ultrasonic impact treatment. *J Constr Steel Res* 233, 109666 (2025). https://doi.org/10.1016/j.jcsr.2025.109666
22. Michalski, M., Piott, F. & Merklein, M. Compression testing of martensitic stainless steel with superimposed ultrasonic vibration. *Procedia Eng* 207, 1970-1975 (2017). https://doi.org/10.1016/j.proeng.2017.10.1100
23. Malygin, G.A. Acoustoplastic effect and the stress superimposition mechanism. *Phys Solid State* 42, 72–78 (2000). https://doi.org/10.1134/1.1131170
24. Siu, K.W. & Ngan, A.H.W. Understanding acoustoplasticity through dislocation dynamics simulations. *Philos Mag* 91(34), 4367-4387 (2011). https://doi.org/10.1080/14786435.2011.606237

25. Wang, Y.L., Zhu, Y.L. & Cai, Z.H. Gradient layer of ultrafine equiaxed grains produced by ultrasonic energy accelerated dynamic recrystallization. *Mater Sci Eng A* 795, 139958 (2020). https://doi.org/10.1016/j.msea.2020.139958
26. Hu, J., Shimizu, T., Yoshino, T., et al. Evolution of acoustic softening effect on ultrasonic-assisted micro/meso-compression behavior and microstructure. *Ultrasonics* 107, 106107 (2020). https://doi.org/10.1016/j.ultras.2020.106107
27. Kuz'min, E.V., Lysak, V.I., Kuz'min, S.V., et al. Influence of structure formation and properties of bimetal produced by ultrasound-assisted explosive welding. *J Manuf Process* 71, 734-742 (2021). https://doi.org/10.1016/j.jmapro.2021.10.006
28. Lysak V.I., Kuz'min S.V. Energy balance during explosive welding. J Mater Process Technol 222, 356-364 (2015). https://doi.org/10.1016/j.jmatprotec.2015.03.024
29. Qingyu, W., Xuedao, S., Yusen, C., et al. Hot Deformation Behavior and Dynamic Recrystallization Model of 7075-T6 Aluminum Alloy. *J Mater Eng Perform* (2025). https://doi.org/10.1007/s11665-025-12919-3
30. Cao, M.Y., Hu, H., Jia, X.D., et al. Mechanism of ultrasonic vibration assisted upsetting of 6061 aluminum alloy. *J Manuf Process* 59, 690-697 (2020). https://doi.org/10.1016/j.jmapro.2020.09.070
31. Zhou, H., Cui, H., Qin, Q., et al. A Comparative Study of Mechanical and Microstructural Characteristics of Aluminium and Titanium Undergoing Ultrasonic Assisted Compression Testing. *Mater Sci Eng A* 682, (2016). https://doi.org/10.1016/j.msea.2016.11.021
32. Hu, J., Shimizu, T., Yoshino, T., et al. Ultrasonic dynamic impact effect on deformation of aluminum during micro-compression tests. *J Mater Process Technol* 258, 144-154 (2018). https://doi.org/10.1016/j.jmatprotec.2018.03.021
33. Wright, S. & Nowell, M. EBSD image quality mapping. *Microsc Microanal* 12, 72-84 (2006). https://doi.org/10.1017/S1431927606060090
34. Liu, M., Roven, H.J., Liu, X., et al. Grain refinement in nanostructured Al–Mg alloys subjected to high pressure torsion. *J Mater Sci* 45, 4659–4664 (2010). https://doi.org/10.1007/s10853-010-4604-3
35. Yang, B., Gao, M., Wang, Y., et al. Dynamic recrystallization behavior and mechanical properties response of rheo-extruded Al–Mg alloys with various Mg contents. *Mater Sci Eng A* 849, 143450 (2022). https://doi.org/10.1016/j.msea.2022.143450

36. Yao, N. & Wang, Z. Handbook of Microscopy for Nanotechnology (2005). https://doi.org/10.1007/1-4020-8006-9